Available online at www.sciencedirect.com
SCIENCE DIRECT®
Journal of Non-Crystalline Solids 351 (2005) 863–868
JOURNAL OF NON-CRYSTALLINE SOLIDS
www.elsevier.com/locate/jnoncrysol

Characterization of rare earth aluminosilicate glasses

J. Marchi [a], D.S. Morais [a], J. Schneider [b], J.C. Bressiani [a], A.H.A. Bressiani [a,*]

[a] *Instituto de Pesquisas Energéticas e Nucleares, Centro de Ciência e Tecnologia de Materiais, Av. Prof. Lineu Prestes, 2242-Cidade Universitária, 05508-000 São Paulo, SP, Brazil*
[b] *Universidade de São Paulo Instituto de Física de São Carlos, Laboratório de Ressonância Magnética, Av. Dr. Carlos Botelho 1465, 13560-970 São Carlos, SP, Brazil*

Received 16 July 2004; received in revised form 21 December 2004
Available online 23 March 2005

Abstract

Rare earth glasses are commonly used in lasers, sensors and radiation shield glasses. Rare earth aluminosilicate-based glasses have been successfully used as in vivo radiation delivery vehicles, in treatment of primary hepatocellular carcinoma, irradiation of diseased synovial membrane for the treatment of rheumatoid arthritis, and treatment of prostate tumors. These glasses have also been found useful to promote liquid-phase sintering of covalent ceramics and, specifically, silicon carbide-based ceramics. Usually, the SiO_2–Al_2O_3–RE_2O_3 system is used as sintering additives. In this work, several rare earth silicate glasses (RE = Y, La, Nd, Dy and Yb) were prepared based on 60%SiO_2–20%Al_2O_3–20%RE_2O_3 (mol%) compositions. These glasses were characterized by infrared spectroscopy and nuclear magnetic resonance. Moreover, the liquid phase sintering of silicon carbide ceramics was studied using dilatometric experiments with 10 vol.% additives of the 60%SiO_2–20%Al_2O_3–20%RE_2O_3 system.

PACS: 81.05.Kf; 87.64.Hd; 81.05.Je

1. Introduction

Rare earth glasses are used in lasers, sensors, radiation shield glasses and in other uses due to their optical and magnetic properties [1–3]. The properties of rare earth aluminosilicate glasses include [1,2] greater glass transition temperatures, greater hardness and elastic modulus, and greater chemical durability than many other glass compositions. Rare earth aluminosilicate-based glasses have been successfully used as a laser ion hosts, optical lenses, seals, and as in vivo radiation delivery vehicles [4–6]. In this type of application, glasses should be biocompatible, non-toxic and chemically insoluble, to prevent radioactivity leakage within the in vivo treatment site. Additionally, yttrium glasses, in the form of microspheres or seeds, have received attention in treatment of primary hepatocellular carcinoma, irradiation of diseased synovial membrane for the treatment of rheumatoid arthritis, and treatment of prostate tumors [6].

The structural role of ions in aluminosilicate glasses is determined by their size (which controls their coordination number) and by their charge (which controls the strength of the bonds formed to the neighboring anions) [5]. The rare earth ions, due to their size, are able to occupy octahedral sites in the glass structure (instead of tetrahedral ones), in which the bonds between rare earth ions and surrounding oxygens are the weakest links in the glass structure compared to Al–O or Si–O bonds.

* Corresponding author. Tel.: +55 11 3816 9363; fax: +55 11 3816 9370.
E-mail addresses: jmarchi@ipen.br (J. Marchi), abressia@ipen.br (A.H.A. Bressiani).

0022-3093/$ - see front matter © 2005 Elsevier B.V. All rights reserved.
doi:10.1016/j.jnoncrysol.2005.01.078

The stronger the rare earth–oxygen bonds, the higher the glass transformation temperature, suggesting that rare earth ions act similarly to aluminum ions in these glasses [5].

The bonding conditions of [SiO_4] tetrahedra in rare earth aluminosilicate glasses can be analysed by infrared [7] and nuclear magnetic resonance spectroscopy [8]. Lin and Hwang [4] have concluded from NMR studies of (CeO_2–Al_2O_3–SiO_2) glasses that the aluminum ions exist in Al(4) and Al(6) coordination, depending upon the glass composition. The Al(4)'s are network former, like silicon ions, while the Al(6)'s are network modifiers. Only the network modifier ions could be able to create non-bridging oxygens. It has been reported [9] that in yttrium and lantanium aluminosilicate glasses the tends to adopt fourfold coordination.

Rare earth aluminosilicate-based glasses have also been found useful to promote liquid-phase sintering of silicon carbide-based ceramics [10–15]. In these systems, an oxide powder mixture based on SiO_2–Al_2O_3–RE_2O_3 system forms a liquid at high temperatures. On cooling, some compositions in these rare earth systems can be solidified without crystallization [14], staying within the glass-forming region of the phase diagram, typically within the SiO_2-rich region. The glass-forming region shrinks toward 60%SiO_2–20%Al_2O_3–20%RE_2O_3 compositions as the rare earth ionic radius decreases [15]. The composition and the volume fraction of this glassy phase, along other crystalline secondary phases, affects the microstructure and, thus, the properties of silicon carbide based ceramics.

The aim of this work is to investigate some characteristics of rare earth aluminosilicate glasses (RE = Y, La, Nd, Dy, Yb) based on infrared spectrometry and ^{29}Si and ^{27}Al nuclear magnetic resonance, as well as to observe the sintering of silicon carbide with such additives.

2. Experimental procedure

The starting raw materials used to produce the rare earth aluminosilicate glasses were alumina (A16 SG, Alcoa), silica (Fluka) and rare earth oxides (RE = Y, La, Nd, Dy, Yb, Sigma Aldrich). These rare earth oxides were used to evaluate the influence of the ionic radius of the RE ions on some properties of rare earth aluminosilicate glasses. The powders were characterized for phase composition by X-ray diffraction. Several compositions, containing 60 mol% SiO_2, 20 mol% Al_2O_3 and 20 mol% RE_2O_3 (RE = Y, La, Nd, Dy, Yb) were mixed in an attritior mill for 4 h, dried in a rotoevaporator and melted in air, in a platinum crucible at 1500 °C/1 h. Then, the materials were poured on stainless steel plates to solidify.

Glass densities were measured by the Archimedes method. High-resolution nuclear magnetic resonance (NMR) experiments were carried out at a magnetic field of 9.4 T on a Varian Unity Inova spectrometer. Samples were spun up to 7 kHz in zirconia and silicon nitride rotors. For ^{29}Si-NMR, $\pi/2$ pulses of 3.5 μs were applied and recycle delays as long as 600 s were used to avoid appreciable saturation. Up to 128 transients were collected. For ^{27}Al-NMR, short pulses ($\pi/30$) were applied to produce excitation independent of the quadrupolar coupling. Delays of 1 s were used and 1000 transients were collected. Chemical shifts of ^{29}Si and ^{27}Al were referenced with respect to a kaolinite sample (−91.5 pp) and an aqueous solution of $Al_2(SO_4)_3$ (0 ppm), respectively. Due to the electronic paramagnetism in Dy and Nd glasses, high-resolution NMR experiments were carried out only in La and Y glasses.

Infrared absorption spectra of rare earth aluminosilicate glasses were measured using a Fourier transform infrared spectrometer and the KBr method (ratio of 1 part of powder mixture:1 part of KBr). The spectra were measured in 450–4000 cm^{-1} region.

The liquid phase sintering of silicon carbide ceramics was studied through dilatometric experiments. Ninety vol.% of silicon carbide powder (BF 17, 91.9% β-SiC, H.C. Starck) was mixed in the attritor together with 10 vol.% of additives, in the same composition of the rare earth aluminosilicate glasses. The slurries were dried in a rotoevaporator and the powders were uniaxially and then cold isostatically pressed at 200 MPa. Sintering was performed in a dilatometer (Netzsch, E7, 402 DL). Linear shrinkage and linear shrinkage rate were obtained and the effect of the rare earth element was studied.

3. Results

X-ray diffraction analysis of the raw materials shows that all powders used were completely crystalline, characterized by narrow diffraction peaks. The oxide phases were the only ones present in the powders. X-ray diffraction analysis of the rare earth aluminosilicate glasses indicates the amorphous character, as expected.

Densities of aluminosilicate glasses are listed in Table 1. We observed, as predicted in literature, that densities increases as the rare earth element ionic radius (except yttria-glass) diminish, due to increasing atomic weight.

The ^{27}Al NMR spectra from La and Y glasses are shown in Fig. 1. The NMR peaks partially resolved correspond to Al in coordination VI, V and IV. The positions of these peaks and their attribution to the coordination numbers, in accordance to literature [8,17], are shown in Table 2. The Al(IV) lines are better resolved in both spectra, with peaks at 54.5 ppm and 54.7 ppm for Y and La glasses, respectively. The peak at 33.5 ppm in the Y-glass and the asymmetry around 30 ppm in the La-glass can be attributed to Al(V).

Table 1
Characteristics of materials

Element	Weight (u.m.a.)	Ionic radius (A) RE^{+3} [16]	RE_2O_3 density (g/cm^3)	Glass density (g/cm^3)
Y	88.9	0.88	5.01	3.48 ± 0.02
La	139.9	1.040	6.51	3.84 ± 0.02
Nd	144.2	0.985	7.24	3.89 ± 0.02
Dy	162.2	0.908	7.81	4.19 ± 0.02
Yb	173.0	0.858	9.17	–

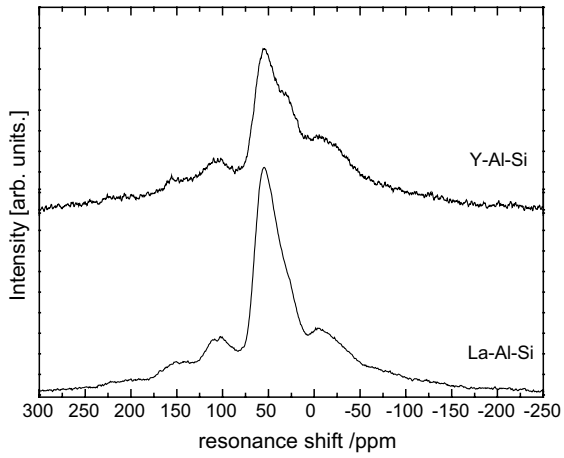

Fig. 1. ^{27}Al NMR spectra of yttrium and lantanium aluminosilicate glasses.

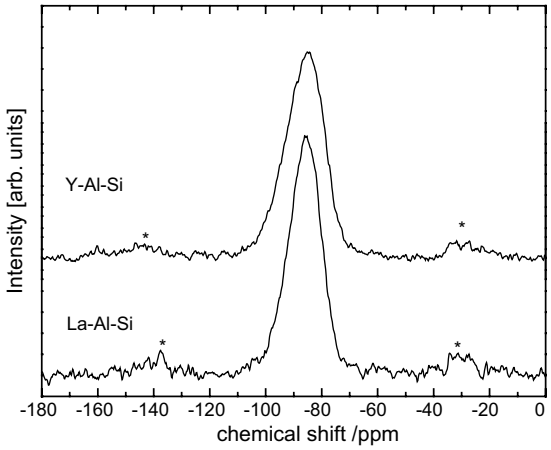

Fig. 2. ^{29}Si NMR spectra of yttrium and lantanium aluminosilicate glasses.

Table 2
Parameters of ^{29}Si-NMR and ^{27}Al-NMR peaks

Rare earth in aluminosilicate glasses	Parameters of ^{29}Si-NMR peaks (ppm)			Positions of ^{27}Al-NMR peaks (ppm)		
	Chemical shifts for the maximum	First moment	Line breath	Al(IV)	Al(V)	Al(VI)
Y	−85.1 ± 0.1	−86.8 ± 0.2	15.9 ± 0.2	54.5 ± 0.2	33.5 ± 0.5	−7.0 ± 0.5
La	−86.1 ± 0.1	−86.0 ± 0.2	13.6 ± 0.2	54.7 ± 0.2	30 ± 1	−5.0 ± 0.5

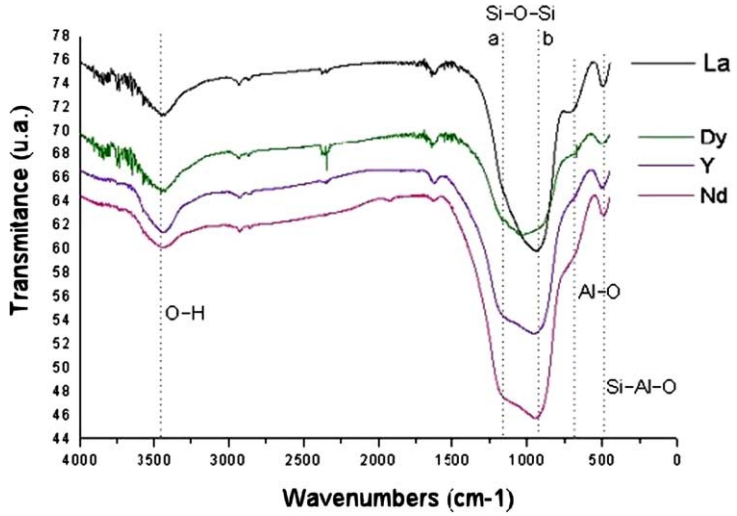

Fig. 3. Infrared transmittance spectra of rare earth aluminosilicate glasses (RE = Y, La, Nd, Dy), (a) one non-bridging oxygen in Si–O, (b) two non-bridging oxigen in Si–O.

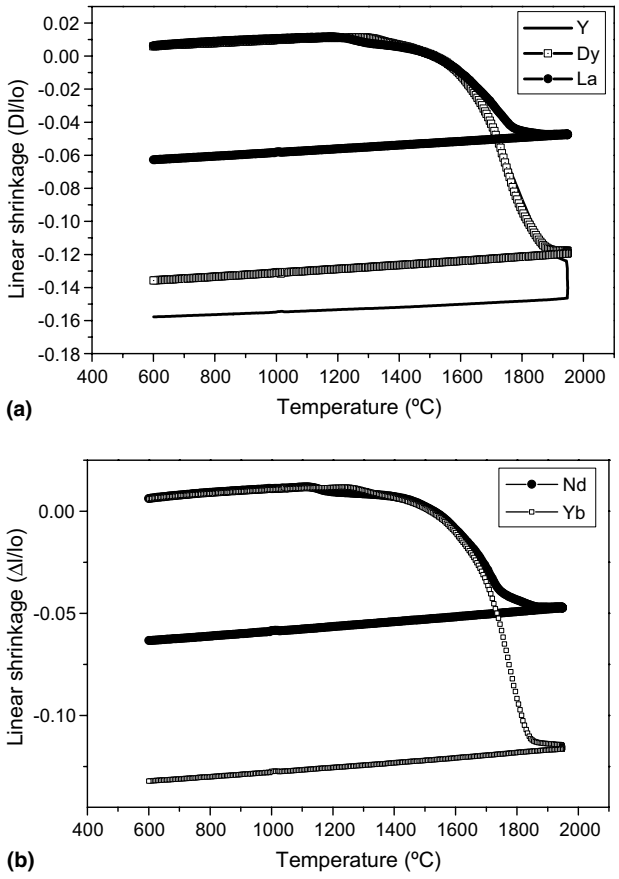

Fig. 4. Linear shrinkage of silicon carbide containing 10 vol.% of additives based on 60 mol% SiO_2–20 mol% Al_2O_3–20 mol% RE_2O_3 compositions (RE = Y, La, Nd, Dy, Yb).

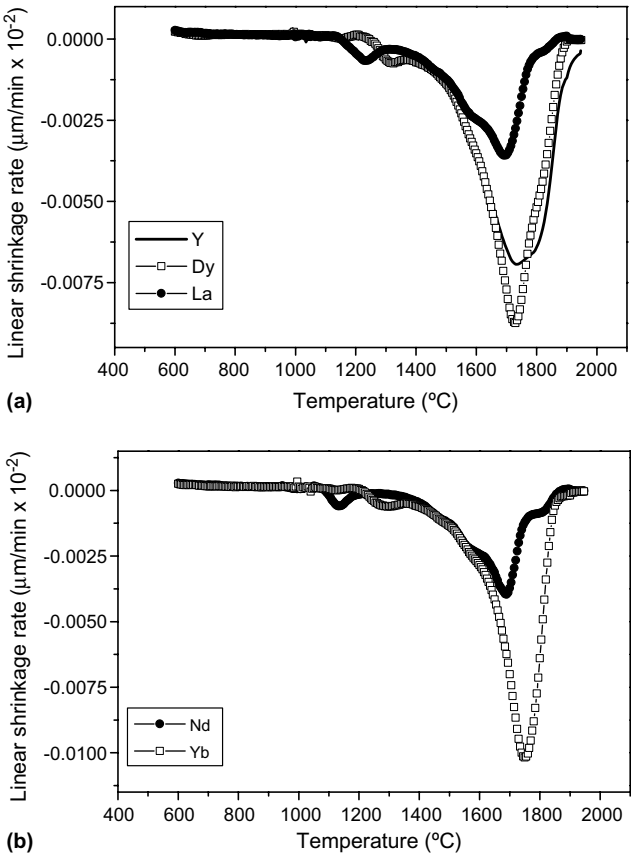

Fig. 5. Linear shrinkage rate of silicon carbide containing 10 vol.% of additives based on 60 mol% SiO_2–20 mol% Al_2O_3–20 mol% RE_2O_3 compositions (RE = Y, La, Nd, Dy, Yb).

The broad bands in −7 ppm and −5 ppm in Y and La glasses respectively correspond to Al(VI).

The ^{29}Si NMR spectra from La and Y glasses are shown in Fig. 2. For each glass, there is a single broad NMR line spanning the chemical shift range of several $Q^n(m\mathrm{Al})$ silicate units. The chemical shifts for the maximum, the first moment and line breadth of the NMR peaks are indicated in Table 2.

The infrared spectrum (Fig. 3) show that rare earths have a considerably influence on glass structure. In the 1250–750 cm^{-1} region, two bands (1165 and 943) are observed. These bands are related to the number of non-bridging oxygens and to the rare earth element ionic radius. The 1165 cm^{-1} band (a), containing up to 1 non-bridging oxygen (NBO) increases in intensity as the rare earth ionic radius decreases. The 943 cm^{-1} band (b), with two non-bridging oxygen, decreases in intensity.

In the 450–750 cm^{-1} region, another two bands are observed. The first one, in 682 cm^{-1} is related to stretching vibration of the Al–O bond with aluminum ions in Al four coordination [7]. These results are in good agreement with NMR spectra. The later, in 494 cm^{-1}, is related to the bending vibrations of Si–Al–O linkages.

The linear shrinkage data from dilatometric measurements (Fig. 4) reveal that at 1950 °C, there is no shrinkage, except in yttria samples. Lantanium and neodimium yield smaller linear shrinkage and the process ends at approximately 1800 °C. The respective linear shrinkage rate (Fig. 5) indicates that such change is related to the rare-earth oxide additive.

4. Discussion

The results based on X-ray diffraction analysis show that temperature/time conditions were suitable to obtain the rare earth glasses, except for ytterbium oxide. The composition containing 60 mol% SiO_2, 20 mol% Al_2O_3 and 20 mol% Yb_2O_3, molten at 1500 °C/1 h, had such a larger viscosity that it subsequently crystallized when poured, even in a fast process. As a result, ytterbium aluminosilicate glasses were not obtained. Moreover, traces of La_2O_3 as a crystalline phase were detected in lantanium aluminosilicate glasses.

The ^{27}Al NMR spectra are in agreement with similar experiments reported in the literature [2,8,9]. The accurate quantification of the fraction of Al in these sites is not possible due to the partial overlap of spinning sidebands, especially from the strong Al(IV) line over the Al(VI) line. However, a qualitative comparison between the spectra of both glasses can be made.

From the direct inspection of the NMR spectrum (Fig. 1), we infer that the dominant coordination of Al in La-glass is fourfold. This situation is different for Y-glass, where the three kinds of coordination are appreciably populated. Also, the line-widths of the NMR peaks of the Y-glass are greater than those of the La-glass, indicating a greater distribution of nuclear interaction parameters as the isotropic chemical shift and the quadrupolar coupling constant for each kind of coordination. This fact indicates a larger distribution of local structural arrangements around Al in Y-glasses compared those of La-glasses. The positions of the NMR peaks show little variation between the glasses, indicating similarities between the mean atomic environments in both glasses. As can be seen in Table 2, this coincidence is more evident for the Al(IV) sites. This is expected from the greater strength of the Al–O bonds in tetrahedral coordination with respect to higher coordinations, giving rise to a more rigid structure around the Al^{3+} ion. In summary, ^{27}Al-NMR indicates that Al atoms are preferentially acting as network former species in La-glass, and the structural environments are more uniform compared to those in Y-glass.

As it is well-known, the ^{29}Si chemical shift in silicates is sensitive to the number, n, of bridging oxygens as well as the number m of those forming Si–O–Al bonds [8]. Therefore, there are many possible $Q^n(m\mathrm{Al})$ silicates with chemical shifts in the observed spectral range (Fig. 2) and, having no well resolved peaks, a quantitative numerical fitting of these lines to the NMR spectrum is impossible. However, some conclusions can be drawn considering the asymmetry of the measured NMR lines.

According to Table 2, the ^{29}Si-NMR line of La-glass is narrower and more symmetric than the line in the spectrum of Y-glass. The line-width for the La-glass is less than for the Y-glass, indicating a smaller dispersion for the distribution of atomic environments of silicon. Also, for the La-glass, the chemical shifts corresponding to the peak position δ_{max} and first moment δ_{med} are the same (−86 ppm). For the Y-glass, the δ_{max} is shifted to less shielded values (−85.1 ppm) while the mean δ_{med} is shifted to more shielded values (−86.8 ppm). This asymmetry is caused by the increment of the NMR intensity in the more shielded edge of the Y spectra (−110 ppm to −100 ppm), which is associated with silicates Q^4, Q^4(1Al) and, with less probability, Q^3. From this observation, it is possible to conclude that the silicate network in Y-glass has a larger degree of connectivity with respect to the La-glass.

These infrared results (Fig. 3) are in good agreement with the viscosity during the glass preparation. Lantanium aluminosilicate glass were easily refined and poured. Disprosia aluminosilicate glass required a longer fining time, with some bubbles retained in the glass. Due to the greater viscosity of ytterbium aluminosilicate glass, these could not be poured and became crystalline inside the platinum crucible.

It can be seen that the ratio of intensities I_b/I_a between bands of 2-NBO (Q^2) to 1-0-NBO (Q^4, Q^3) is larger in the La-glass with respect to the Y glass. This observation is in agreement with the NMR results. The ^{29}Si-NMR spectrum of the La-glass was less intense in the Q^4–Q^3 region of silicon chemical shifts, indicating a less interconnected silicate network compared with the Y-glass. Considering the ^{27}Al-NMR spectrum, which shows a greater fraction of Al(IV), we suggest that the reduction in the connectivity of Q^4 and Q^3 silicates in the La-glass can be associated to the formation of Si–O–Al bonds for these tetrahedra. This hypothesis can be justified by considering that a decrease in the number of NBO (i.e. $Q^n \rightarrow Q^{n-1}$) as well as the appearance of Si–O–Al bonds for a fixed n, (i.e. $Q^n \rightarrow Q^n(1\mathrm{Al})$), produce a shift of the silicon resonance to less shielded values, in agreement with the observations in the La-glass spectrum. Therefore, the atomic structure of La-glass can be better represented by a mixed aluminate–silicate network than a separate silicate network of smaller connectivity. Since the intensity ratio, I_b/I_a, for Dy and Nd-glasses are quite similar to the Y-glass, we conclude that, in these three glasses, Al has a limited role as network former and silicates of larger mutual connectivity are present. Of these glasses, the network of the Dy-glass may have the largest silicate connectivity, as follows from the fact that $I_b/I_a \approx 1$.

It is well known that the composition of additives used to help the densification of silicon carbide materials, related to different components and/or the viscosity of a such phase, have a great influence of the sintering process [18,19]. The silicon carbide sintering occurs through liquid phase process [11–13]. In lower temperatures, there is a range of maximum shrinkage rate due to rearrangement of silicon carbide particles as the liquid starts to form. At higher temperatures, the range is less and is related to the solution reprecipitation process [20,21].

We observed in another paper [22] that the existence of only one range of maximum shrinkage rate due to solution reprecipitation process is related to the fact that these compositions are located in the glass forming region, and, consequently, to the absence of secondary crystalline phases, which are an obstacle to the solution reprecipitation process. In this study, we observed that samples containing lanthania or neodimia as additives have extra ranges of maximum shrinkage rate (Fig. 5),

which we suggest in these compositions, are transient secondary crystalline phases formation, such as rare-earth silicates at low temperatures. These phases can dissolve into the liquid, and can disappear or crystallize as other phases, such as rare earth aluminum rich phases [23]. These phases are responsible for hindering the solution–reprecipitation process [22]. Samples containing yttria, dysprosia and ytterbia have only one range of maximum shrinkage rate due to a solution–reprecipitation process, and, probably, no transient secondary crystalline phases. Considering the several rare-earths used, we suggest that Y, Dy and Yb aluminosilicate samples are located inside the glass forming region (established at 1700 °C/1 h), while La and Nd samples are located out of this region.

5. Conclusion

From the structural point of view, it is possible to conclude that the La-glasses have a mixed silica–alumina network. Silicate groups are dispersed, having low mutual connectivity, mainly as Q^2. For the other glasses, the network is formed mainly by the silicate groups and Al^{3+} ions act preferentially as modifiers, in coordination VI and V. The Dy-glass has the network with the largest silicate connectivity of these glasses.

Considering the silicon carbide based ceramics, we concluded that Y, Dy and Yb aluminosilicate samples are located inside the glass forming region, perhaps due to a greater wettability in these ceramics than for La and Nd-samples.

Acknowledgments

The authors would like to thank CNPq, FAPESP and PRONEX/FINEP for financial support, and Laboratório de Materiais Vítreos, DEMa, UFSCar.

References

[1] H. Lemercier, T. Rouxel, D. Fargeot, J.L. Besson, B. Piriou, J. Non-Cryst. Solids 201 (1996) 128.
[2] N.J. Clayden, S. Esposito, A. Aronne, P. Pernice, J. Non-Cryst. Solids 258 (1999) 11.
[3] A.G. Clare, in: J.E. Shelby (Ed.), Rare Elements in Glasses, Key Eng. Mater., vol. 94&95, Trans Tech Publications, Switzerland, 1994, p. 161.
[4] S.L. Lin, C.S. Hwang, J. Non-Cryst. Solids 202 (1996) 61.
[5] J.E. Shelby, J.T. Kohli, J. Am. Ceram. Soc. 73 (1990) 39.
[6] J.E. White, D.E. Day, in: J.E. Shelby (Ed.), Rare Elements in Glasses, Key Eng. Mater., vol. 94&95, Trans Tech Publications, Switzerland, 1994, p. 181.
[7] J.T. Kohli, R.A. Condrate, J.E. Shelby, Phys. Chem. Glasses 34 (1993) 81.
[8] J.T. Kohli, J.E. Shelby, J.S. Frye, Phys. Chem. Glasses 33 (1992) 73.
[9] T. Schauller, J.F. Stebbins, J. Phys. Chem. B 102 (1998) 10690.
[10] M. Keppeler, H.G. Reichert, J.M. Broadley, G. Thurn, I. Wiedmann, J. Euro. Ceram. Soc. 18 (1998) 521.
[11] F.K. Van Dijen, E. Mayer, J. Euro. Ceram. Soc. 16 (1996) 413.
[12] V.A. Izhevskyi, La.A. Genova, A.H.A. Bressiani, J.C. Bressiani, Mater. Res. 4 (2000) 131.
[13] Y.M. Chiang, D.P. Birnie III, W.D. Kingery, Physical Ceramics, John Wiley, EUA, 1997.
[14] I.H. Arita, D.S. Wilkinson, G.R. Purdy, J. Am. Ceram. Soc. 75 (1992) 3315.
[15] J.E. Shelby, in: J.E. Shelby (Ed.), Rare Elements in Glasses, Key Eng. Mater., vol. 94&95, Trans Tech Publications, Switzerland, 1994, p. 1.
[16] S.J. Schneider, Engineering Materials Handbook, vol. 4. Ceramics and Glasses, ASM International, 1995.
[17] G. Engelhardt, D. Michel, High Resolution Solid-state NMR of Silicates and Zeolites, John Wiley, Norwich, 1987.
[18] T. Grande, H. Sommerset, E. Hagen, K. Wiik, M.A. Einarsrud, J. Am. Ceram. Soc. 80 (1997) 1047.
[19] H. Xu, T. Bhatia, A.S. Deshpande, P.N. Padture, J. Am. Ceram. Soc. 84 (2001) 1578.
[20] H.J. She, K. Ueno, Mater. Res. Bull. 34 (1999) 1629.
[21] Y. Zhou, K. Hirao, M. Toriyama, S. Kanzaki, J. Am. Ceram. Soc. 84 (2001) 1642.
[22] J. Marchi, J.C. Bressiani, A.H.A. Bressiani, Mater. Res., submitted for publication.
[23] T.I. Mah, K.A. Keller, S. Sambasivan, R.J. Kerans, J. Am. Ceram. Soc. 80 (1997) 874.